Accepted Manuscript

Ongoing Lung Inflammation and Disease Progression in Mice after Smoking Cessation Beneficial Effects of Formyl-Peptide Receptor Blockade

Giovanna De Cunto, Barbara Bartalesi, Eleonora Cavarra, Emilia Balzano, Giuseppe Lungarella, Monica Lucattelli

PII: S0002-9440(18)30038-5

DOI: 10.1016/j.ajpath.2018.06.010

Reference: AJPA 2938

To appear in: *The American Journal of Pathology*

Received Date: 15 January 2018

Revised Date: 4 June 2018

Accepted Date: 18 June 2018

Please cite this article as: De Cunto G, Bartalesi B, Cavarra E, Balzano E, Lungarella G, Lucattelli M, Ongoing Lung Inflammation and Disease Progression in Mice after Smoking Cessation Beneficial Effects of Formyl-Peptide Receptor Blockade, *The American Journal of Pathology* (2018), doi: 10.1016/j.ajpath.2018.06.010.

Ongoing lung inflammation and disease progression in mice after smoking cessation: Beneficial effects of formyl-peptide receptor blockade

Giovanna De Cunto, Barbara Bartalesi, Eleonora Cavarra, Emilia Balzano, Giuseppe Lungarella and Monica Lucattelli

Department of Molecular and Developmental Medicine, University of Siena, Via Aldo Moro n.2, 53100 Siena, Italy

number of text pages: 27

number of tables: 3

number of figures: 7

Running Head: Inflammation after smoking cessation.

Funding: Supported by grants from MIUR, Rome, Italy (PRIN: prot. 2008T5BLWA), and the University of Siena, Italy (PAR grant 122004).

Name and address of the corresponding author:

Monica Lucattelli, PhD, Department of Molecular and Developmental Medicine, University of Siena, via Aldo Moro n. 2, 53100 Siena, Italy.

Telephone: +39 0577 234024; email: monica.lucattelli@unisi.it

Disclosures: None declared.

Abstract

The most important risk factor for chronic obstructive pulmonary disease (COPD) is cigarette smoking. Until now, smoking cessation (SC) is the only treatment effective in slowing down the progression of the disease. However, in many cases SC may only relieve the airflow obstruction and inflammatory response. Consequently, a persistent lung inflammation in ex-smokers is associated with progressive deterioration of respiratory functions. This is an increasingly important clinical problem whose mechanistic basis remains poorly understood. Available therapies do not adequately suppress inflammation and are not able to stop the vicious cycle that is at the basis of persistent inflammation. Also in mice after SC an ongoing inflammation and progressive lung deterioration is observed. After four months of smoke exposure mice show mild emphysematous changes. Lung inflammation is still present after SC and emphysema progresses during the following six months period of observation. Destruction of alveolar walls is associated with airways remodelling (goblet cell metaplasia and peribronchiolar fibrosis). Modulation of formyl-peptide receptor signalling with antagonists mitigates inflammation and prevents deterioration of lung structures. This study suggests an important role for N-formylated peptides in the progression and exacerbation of COPD. Modulating formyl-peptide receptor signal should be explored as potential new therapy for COPD.

Introduction

Chronic obstructive pulmonary disease (COPD) is characterized by progressive obstruction of airflow, not fully reversible, which is accompanied by a chronic inflammatory response, induced by deleterious particles or gases, in airways and lung parenchyma (1). The most important risk factor for COPD is cigarette smoking (2). COPD is a collection of conditions, which include emphysema, chronic bronchitis with mucus hyper-secretion, bronchiolar and vascular remodelling, and sometimes the presence of fibrotic areas scattered throughout the parenchyma, in which emphysema and fibrosis may coexist. There are currently no specific COPD treatments and smoking cessation remains the most effective therapeutic intervention in patients with COPD (3). However, in many cases smoking cessation may only relieve the airflow obstruction and inflammatory response (4, 5). Several studies in humans and animal experiments have demonstrated that, once COPD is initiated, the pulmonary inflammatory response continues (5-7) and the enlarged alveolar airspace cannot be reversed following smoking cessation (8). Thus, persistent lung inflammation associated with a progressive deterioration of respiratory function (progressive decline in FEV1) and infections in ex-smokers is an increasingly important clinical problem whose mechanistic basis remains poorly understood.

Studies on mouse models of cigarette smoke identified several mechanisms by which COPD lesions may be induced (9, 10). These include the activation of the innate and adaptive immune responses (11, 12) that can lead enhanced protease/antiprotease (13, 14) or oxidant/antioxidant imbalances (15-17) in lung tissue with alveolar wall degradation.

The precise relationship between smoking, immune modulation in the lung and respiratory infections is still object of investigation since bacterial and viral infections may be critical in the induction of acute exacerbations in later COPD stages (18).

In general, available therapies do not adequately suppress inflammation, and even inhaled corticosteroids, although very effective in asthma, reduce exacerbations only to a certain extent in COPD and do not seem to reduce disease progression (19). Additionally, new classes of drugs, such as phosphodiesterase-4 inhibitors, can prolong the time between re-exacerbations (20) but are not potentially able to stop the vicious cycle at the basis of persistent inflammation that characterizes and influences the various clinical stages of the disease.

Much of the current knowledge on the pathogenic mechanism(s) implicated in COPD derives from studies performed on several experimental animal models and in particular on smoking mice, which are able to replicate several features of human COPD (10, 21, 22, 23). Recently, we demonstrated that genetic ablation of formyl-peptide receptor-1 (FPR-1) gene in mice or treatment with specific antagonists of FPRs prevents recruitment of inflammatory cells in the lung and confers protection from smoking-induced lung emphysema (24). These receptors, over-expressed in patients with COPD (25), have been recently involved, together with mitochondrial formylated peptides, also in acute lung inflammation and injury (26).

In this context, by using a "curative" experimental model of CS-induced pulmonary changes that is currently used in pre-clinical studies (27) we studied the ongoing lung inflammation and deterioration that follows smoking cessation as well as the role of (FPR) signalling in the persistency of inflammation. The modulation of FPR-related signalling in mice halts chronic inflammation and prevents the deterioration of alveolar structures and the remodelling of airways that follow smoking cessation in mice. It is widely accepted that the enlargement of alveolar airspaces and the remodelling

of small airways induced by cigarette smoke constitute the pathological basis of airflow obstruction in COPD patients (28, 29).

Materials and Methods

Animal Experiments

Male C57Bl/6 mice (4 to 6 wk old) used in this study were purchased from Charles River (Calco, Italy). The mice were housed in an environment controlled for light (7 AM to 7 PM) and temperature (18°C to 22°C); food (Mucedola Global Diet 2018; Harlan, Correzzana, Italy) and water were provided for consumption *ad libitum*. All animal experiments were conducted in conformity with the "Guiding Principles for Research Involving Animals and human Beings" and were approved by the Ethics Committee of the University of Siena.

Exposure to cigarette smoke

Mice from each experimental group were exposed to either room air or to the smoke of three cigarettes/day, 5 days/week for 4-, 6-, 8-, and 10 months, (Virginia filter cigarettes, 12 mg of tar and 0.9 mg of nicotine). The methodology for smoke exposure has previously been described in details (30).

Experimental design

The scheme of animal treatments is reported in Fig. 1. The day of the start of the study was defined as day 0, allowing the association of this time point with the schedule of smoke cessation and compound administration. Several groups of mice were used in this study and sacrificed at 4, 6, 8, and 10 months from the start of the experiment. Group 1 includes control mice exposed to room air.

Group 2 includes mice exposed to cigarette smoke (CS) and then sacrificed at day 8th after 4 months, and at 6, 8, and 10 months from the start of the treatment. Another group of mice (Group 3) was exposed to CS for 4 months and then left to rest after smoking cessation (SC) at room air for the following 2, 4, or 6 months.

Additional two groups of mice were treated at 4 months of CS exposure with the nonselective FPR antagonist Boc2N-t-butoxycarbonyl-Phe-DLeu-Phe-DLeu-Phe-OH (Boc2) (Group 4), or the selective FPR-1 antagonist cyclosporine H (CsH) (Group 5) for the first 3 days after SC, and subsequently sacrificed together with animals of group 1, 2, and 3, at various specified times after SC.

Treatment with FPRs Antagonist Cyclosporine H and Boc2

After four months of CS exposure, a group of mice was treated intraperitoneally (i.p.) twice a day for three consecutive days with 10 µg N-t-butoxycarbonyl-Phe-DLeu-Phe-DLeu-Phe-OH (Boc2) (MP Biomedicals, Santa Ana, CA). As reported in a previous study, inhibitors were dissolved in 50 µL saline containing 7.5% DMSO and 2.5% ETOH (24). A second group of mice was treated with cyclosporine H (CsH) (ENZO Biochem Inc., Farmingdale, New York, NJ) 50 µg in 50 µL saline containing 7.5% DMSO and 2.5% ETOH, given once a day for three consecutive days. After these pharmacological treatments, mice were sacrificed at various times (8 days, 2 or 6 months) from SC.

Morphology and Morphometry

Six mice from each group were anesthetized with sodium pentobarbital, sacrificed by severing the abdominal aorta and the lungs were immediately removed.

Lungs were fixed intra-tracheally with formalin (5%) at a pressure of 20 cm H_2O. Post-fixation lung volume was measured by water displacement. Lungs were processed for histology and lung slides were analyzed for morphology and morphometry. Assessment of emphysema included mean linear intercept (LM) and internal surface area (ISA). (27). For the determination of the LM and ISA two blinded pathologists evaluated 40 histological fields for each pair of lungs, both vertically and horizontally. The development of goblet cell metaplasia was evaluated by periodic acid-Schiff reaction (22, 31). Peribronchiolar fibrosis was quantitated by point counting in paraffin-embedded lung after Masson's trichrome staining (12, 32).

Inflammatory Cells Profile in BALF

The total and differential cell counts in bronchoalveolar lavage fluids (BALFs) were performed in five mice from each group at 4 and 8 months from the start of the study. Before removing lungs, the tracheas were isolated *in situ* in animals under anaesthesia and then cannulated with a 20-gauge blunt needle. With the aid of a peristaltic pump (P-1 Pharmacia), the lungs were lavaged *in situ* three times with 0.6 mL saline solution. The average fluid recovery was greater than 95%.

Immunolocalization of Nuclear Factor-kB (NF-kB)

Immunohistochemical analysis of NF-κB was performed on 5-μm lung sections. Antigen retrieval was performed by heating in a microwave oven for 20 min in 0.01 M citrate buffer at pH 6.0 and allowing slow cooling at room temperature. Successively all sections were incubated for 30 min in cool solution 0.1% citrate sodium containing 0.1% Triton X-100 to facilitate the antibodies accessibility, and then again incubated with 3% bovine serum albumin for 30 min at room temperature to block non-specific antibody binding. All sections were incubated overnight at 4 °C with rabbit anti- NF-κB (1:200, Biolegend Inc., San Diego, CA). The sections were rinsed with PBS and incubated with Alexa Fluor-488-labelled donkey anti-rabbit antibodies (1:200, Molecular Probes, Eugene) for 45 min in the dark and at room temperature. Finally, the sections were incubated with 1μg/mL RNAse for 30 min at room temperature, with 1μg/mL propidium iodide (SIGMA Aldrich, St Louis, MO) for additional 5 min, and then analyzed with a Zeiss LSM 510 META confocal microscope equipped with Kripton/Argon (Kr-Ar) and Helium/Neon (He-Ne) lasers. BP-505-530 and LP 560 emission filters were used to acquire FITC and propidium iodide after 488 and 543 nm excitations. Images captured using a 63x objective and processed with a ZEISS LSM computer software.

RNA isolation and cDNA synthesis

Total RNA was extracted from lungs of mice using TRi Reagent (Ambion, Austin, TX) according to the manufacturer's instructions. Five mice for each group were used for RNA isolation. RNA was re-suspended in reverse transcription-PCR Grade Water (Ambion, Austin, TX) and the amount and purity of RNA was quantified spectrophotometrically by measuring the optical density at 260 and 280 nm. Integrity was checked by agarose gel electrophoresis.

Two micrograms of total RNA was treated with TURBO DNAse (TURBO DNA-free kit, Ambion, Austin, TX) for 30 min and reverse transcribed using the RETROscript kit (Ambion, Austin, TX) according to the manufacturer's instructions. Two hundredths of the final volume of reverse transcription was used for real-time reverse transcription-PCR.

Real-time reverse transcription-PCR

Real-time reverse transcription-PCR was performed in triplicate for each sample on the MJ Opticon Monitor 2 (MJ Research Co., Waltham, MA) with specific locked nucleic acid (LNA) probes from the Mouse Universal Probe Library Set (UPL probes, Roche, Indianapolis, IN).

Primers were designed by using the free online ProbeFinder software that shows a pair of specific primers for each probe from the Universal ProbeLibrary set (Table1). The combination of primers and probes provides specific amplification and detection of the target sequence in the sample.

PCR reactions were performed in a volume of 25 µL and contained 12.5 µL of FastStart TaqMan Probe Master (Roche, Indianapolis, IN), 300 nmol/L forward and reverse primers (TIBMolbiol, Genova, Italy), 200 nmol/L UPL probes, and 5 µL of cDNA.

Reactions were incubated at 95 °C for 10 min and then amplified for 40 cycles, each cycle comprised of an incubation step at 94 °C for 15 s followed by 60 °C for 1 min.

The real-time reverse transcription-PCR assay included a non-template control and a standard curve of four serial dilution points (in steps of 10-fold) of each of the test cDNAs.

The analysis of the results was based on the comparative Ct method (ΔΔCt) in which Ct represents the cycle number at which the fluorescent signal, associated with an exponential increase in PCR products, crosses a given threshold. The average of the target gene was normalized to 18S rRNA as the endogenous housekeeping gene (33).

Quantification of Goblet Cell Metaplasia

The total number of cells, as well as the percentage of PAS-positive cells, was determined in lung tissue sections from six C57BL/6 mice belonging to each group at 10 months from the start of the experiments and from additional six smoking mice at 4 months after smoke exposure. The number of cells in airways that demonstrated PAS staining was determined by examining eight intrapulmonary airways per section, and counting at least 3,000 cells/section (31). Data were reported both as the number of positive cells per millimeter of basement membrane, and as the percentage of positive cells per total cells.

Statistical Analysis

Data are presented as mean ± SD. The significance of the differences was calculated using one-way analysis of variance (F-test). A *P*-value < 0.05 was considered significant.

Results

The morphological response to 4-months exposure to cigarette smoke is characterized by mild emphysematous changes

Histologically, the lungs of the mice exposed to room air for 4 months showed a well-fixed normal parenchyma with normal airways (Fig.2 A). After four months of smoke exposure mice showed foci of mild emphysema disseminated throughout the lung parenchyma (Fig. 2 B).

Accordingly, the lungs from mice exposed to CS at this time showed a low but a significant increase of LM value (+7%, 42.55±1.2 vs 39.82±1.2 µm, $P < 0.05$) (Fig. 2 C) and a significant decrease of ISA value (-10%, 1010±50 vs 1129±35 cm^2, $P<0,05$) when compared to mice belonging to air-control group (Fig. 2 D).

Progression of emphysematous changes over time

No appreciable lung changes were observed in air-exposed control mice at 10 months from the start of the experiment (Fig. 3 A). On the other hand, emphysematous changes in lung parenchyma were evident in mice exposed for 10 months to CS (Fig. 3 B). The emphysematous lesions were characterized by significant higher LM values (+ 14%, $P < 0.05$) and lower ISA values (-12%, $P < 0.05$) than those observed in the group of air-exposed control mice (Fig. 3 F).

To determine whether SC attenuates inflammation and restores lung changes caused by four month–exposure to CS, an additional group of mice exposed for 4 months to CS followed by additional (4 and) 6 months period without cigarette smoke exposure (SC group) was studied.

Of interest, the histological lung sections from the 4-month smoke–exposed mice and allowed to rest for additional 6 months in room air (Fig.3 C) were practically indistinguishable from those of mice exposed for 10 months to cigarette smoke alone (Fig. 3 B). These lungs are characterized by evident foci of emphysema disseminated throughout the lung parenchyma. A similar degree of emphysema in mice subjected to SC (SC group) and those exposed to CS for 10 months (CS10 M) was seen as revealed by the morphometric values reported in Fig. 3 F (LM values: 44.57±1.3 vs 45.78±2.2 µm, NS; ISA values: 947±33 vs 931±47 cm^2, NS, respectively). Thus, lung emphysema in smoking mice still progresses after SC at a similar extent to that of mice which were continuously exposed to CS for 10 months. Therefore, the cessation of smoking in mice followed by 6 months of rest in the room air, however, resulted in a significant increase in the average linear intercept (+ 11%, $P < 0.05$) and a significant decrease in the internal surface area (- 10%, $P < 0.05$) compared to air control mice (Air 10 M). The morphometric values reported in Fig. 3 F confirm that emphysematous changes still progress after SC during the following period of 6 months and that SC alone has no effect on the progression of lung emphysema once alveolar destruction was initiated.

Lung inflammation is still present for long time in mice after smoking cessation

At 10 months following chronic smoke exposure, inflammatory cells are increased in lung tissue (Fig. 4 B) when lung slides are compared to those of mice exposed to room air (Fig. 4 A). The lung changes observed at 10 months in ex-smoking mice after SC are also associated with a persistent accumulation of inflammatory cells in lung tissue (Fig. 4 C). The increased lung cellularity observed in these experimental groups was also seen in BALFs of these mice. Mice exposed to CS for 8 months had a significant increase in total, macrophage, and neutrophil cell counts in BALFs as compared to air-control mice (Table 2). At the same time point, in mice exposed for 4 months to CS and then left to rest for additional 4 months period in room air (SC group), macrophage numbers in BALFs decreased almost to control levels. On the other hand, neutrophil counts partially decreased at 4 months after smoking cessation but failed to

reach control values (Table 2). Thus, in mice exposed to CS for 4 months a significant increase of neutrophil number is still evident after 4 months from SC.

These results indicate that SC in mice is followed by a persistent inflammatory lung response that is associated with the progression of emphysematous lesion.

Chronic lung inflammation is characterized by persistent nuclear factor-kB (NF-kB) activation

NF-kB is a major regulator of innate immunity and its activation results in fairly rapid changes in gene expression. In normal condition, this factor, in its inactive status, can be localized in the cytoplasm of many lung cells by using a rabbit antibody recognizing the p65 (RelA) component of the NF-kB complex (Fig. 5 A). When activated, RelA translocates to the nucleus where it promotes expression of pro-inflammatory molecules.

A positive and persistent reaction for p65/RelA (green reaction) was still observed at 6 months from the start of experiments in the nuclei of several lung macrophages and epithelial cells of smoking mice (Fig. 5B) as well as of ex-smoker mice after SC (Fig. 5 C). The persistent nuclear positive reaction for RelA was accompanied by a significant up-regulation of mRNA of pro-inflammatory cytokines such as *Il6*, MIP-1, KC, and anti-inflammatory *Il10* (Fig. 5 F).

FPR antagonists reduce lung inflammation and prevent the progression of the lung changes after smoking cessation

To stop the vicious cycle that we hypothesise to be the cause of persistent pulmonary inflammation after SC, Boc2 and CsH, two antagonists of FPR-1 and FPR-2, were administered in mice on the first three days after 4 months of CS exposure. These mice were allowed to rest at room air for the following 6 months.

At day 8 after the start of Boc2 or CsH treatment, total and differential cell counts were performed in BALFs of 5 mice for each experimental groups. The results are reported in Table 3.

In the group of mice treated with Boc2 or CsH, cell counts showed a significant decrease of total cell population as compared with ex-smoker mice exposed to CS for 4 months and then allowed to rest for the following 8 days. Of interest, both antagonists led to a significant reduction of neutrophil migration in BALFs as compared to mice exposed to CS for 4 months, which did not receive any pharmacological treatment (Table 3). However, mild increase of neutrophils and lymphocytes was present in mice treated with Boc2 as compared to air-control mice. Therefore, CsH or Boc2 treatment after SC was effective in reducing the migration of neutrophils in BALFs.

The reduction of neutrophilic inflammation with FPR antagonists after SC strongly suggests an important role of FPR signalling in modulating the inflammatory response once lung destruction is already present.

In addition, the histological evaluation of lungs of smoking animals receiving Boc2 or CsH treatment revealed at 6 months after SC a mild deterioration of lung changes (Figs. 3 D and E, respectively) as compared to animals that did not receive any pharmacological treatment during the first days after SC (Fig. 3 C). The morphologic and morphometric assessment of lung changes performed at 6 months after SC confirmed that the attenuation of inflammatory response obtained by the treatment with FPR antagonists favors a mild evolution of lung lesions preventing the deterioration of pulmonary structures which usually follows SC (Fig. 3 F). Of interest, only very few inflammatory cells were present in lung parenchyma of mice receiving a treatment with Boc2 (Fig. 4 D) or CsH (Fig. 4 E). These features were preceded by i) marked and significant reduction of neutrophils in BALFs of mice receiving FPR

antagonists after smoking cessation (Table 3), ii) absence of nuclear reaction for NF-kB (Figs. 5 D and E), and iii) no significant changes in mRNA expression of pro-inflammatory cytokines such as MIP-1, KC, and *Il6* (Fig. 5 F).

Of interest like in SC group, mice receiving FPR antagonists showed an up-regulation of mRNA for the anti-inflammatory cytokine *Il10* (Fig. 5 F).

The reduction of neutrophilic inflammation with the administration of FPR antagonists after SC strongly suggests an important role of FPR signalling in modulating and perpetuating the inflammatory response once lung destruction is already present.

Treatment with FPR antagonists prevents peribronchiolar fibrosis and reduces the number of goblet cells in airways epithelium

Only small amount of collagen is found around bronchioles and distal bronchi of air-control mice at 10 months from the start of the experiments (Fig. 6 A). At the same time point, peribronchiolar regions of lungs from smoking mice as well as from ex-smoker mice after SC showed an increased collagen deposition (Figs. 6 B and D, respectively). The quantification of collagen deposition areas by point counting did not reveal differences, at 10 months from the start of the study, between smoking mice and mice that stop to smoke after 4 months of CS exposure (Fig. 7 A). However, an increased deposition of collagen was observed in the latter group of mice (Fig. 6 D) as compared to that observed at 4 months of CS exposure (Fig. 6 C). On the contrary, minimal differences in morphology and collagen deposition areas quantitation were observed among air-control mice (Fig. 6 A) and mice receiving Boc2 (Fig. 6 E) or CsH (Fig. 6 F). The point counting analysis performed on collagen deposition areas substantiated these observations (Fig. 7 A). Additionally, at 8 months from the start of the study, a significant increase of mRNA expression for arginase-1 (*Arg1*) and fibroblast growth factor-1 (*Fgf1*) was seen in lung samples of smoking as well as ex-smoker mice of SC groups (Fig. 7B). All these gene products are involved in fibrotic reactions.

Goblet cell metaplasia (GCM) in response to smoke treatment was assessed by counting PAS positive cells in mice at 10 months from the start of the experiments. Data were reported both as the number of positive cells per millimeter of basement membrane (Fig. 7 C) and as the percentage of positive cells per total cells (Fig. 7 D). As recognized, control mice practically do not have goblet cells in their bronchi and bronchioles (9), and also at this time PAS staining was absent in the airway epithelium of air-exposed control animals (Fig. 7 E). Quantitation of PAS-positive cells revealed that around 10% of all airway cells in mice smoking for 10 months are goblet cells (Figs. 7 D and F), and, that the extent of goblet cell metaplasia measured as the percentage of PAS-positive cells was quite similar for mice exposed for a period of 4 months to CS (Fig. 7 G) and those exposed for 4 months to CS and then left to rest for additional 6 months period in room air (SC group) (Figs. 7 D and H). In animals exposed to CS, treated with BOC or CsH and left to rest in room air for the following six months we observed a marked significant reduction of PAS-positive cells (Figs. 7 I and J, respectively) with low significant percentage of PAS positive cells in respect to other smoking groups that did not receive pharmacological treatments (Fig. 7 D). The numbers of PAS-positive cells per millimeter basement membrane in each experimental group is reported in Fig. 7 C. The development of GCM is preceded by a significant up-regulation of mRNA for *Il13* and protease-activated receptor-1 (Par1) coded by *F2r* gene (Fig. 7 B). Both factors implicated in this “adaptive” tissue differentiation.

Discussion

Several studies in humans and animal experiments have demonstrated that, once COPD is initiated, the pulmonary inflammatory response continues (5-7) and the enlarged alveolar airspace cannot be reversed following smoking cessation. Available therapies do not adequately suppress inflammation and are not able to stop the vicious cycle that is at the basis of persistent inflammation.

In this study we demonstrate that also in mice chronically exposed to CS, lung inflammation persists after smoking cessation and is associated with a progressive alveolar loss and remodelling of respiratory tract characterized by the onset of bronchial and bronchiolar goblet cell metaplasia and peribronchiolar fibrosis. Persistent inflammation is characterized in these mice by an increased cellularity with a significant increase of neutrophils and macrophages in the peripheral structure of the lung and a persistent activation of NF-kB associated with a nuclear localization of the p65 (RelA) component of the complex that modulates target genes transcription. In particular, RelA can enhance the transcription of a series of downstream target genes (34) such as pro- or anti-inflammatory cytokines and chemokines (ie, KC, MIP-1beta, IL-6, and IL-10) or enzymes (such as MMP-12, Arginase 1) and factors (ie, FGF-1, PAR-1, and IL-13), which have been implicated in alveolar destruction or in peribronchiolar and bronchial remodelling.

In particular, up-regulation of genes encoding the attractants CXCL1/KC (the murine IL-8 homolog) (35) and CCL4/MIP-1beta (36) would explain the prolonged presence of PMNs and macrophages in peripheral lung structures of mice after SC, whereas the increased expression of Arginase 1 and FGF-1 (37, 38) could explain the consistent collagen deposition in peribronchiolar areas. Additionally, the strong MMP-12 expression coincided with the progression phase of the disease probably for enzyme destruction of alveolar structures by macrophages (39). A link between PAR-1 and IL-13 overexpression and development of GCM may be postulated on the basis of our recent work and other ones published in this matter (31, 40).

Of importance, the modulation of FPR-related signalling in mice by using FPR inhibitors halts chronic inflammation and prevents the deterioration of pulmonary structures that follow smoking cessation.

N-formyl peptide receptors (FPRs) belong to the family of pattern recognition receptors, G-protein–coupled receptor (GPCR) family that regulate innate immune responses (41). Three FPRs have been identified in humans: FPR-1, FPR-2, and FPR-3, which have been described across several species, including mouse. Distinct to the other member of FPR family, the function of FPR-3 remains relatively poorly understood. FPR-1 and FPR-2 have diverse roles in the initiation, propagation, and resolution of inflammation (42). Murine orthologs of human FPR-1 and FPR-2, share a relative high sequence homology, are expressed on similar cell types (neutrophils, macrophages, monocytes, fibroblasts, epithelial, and endothelial cells), and induce same effects of neutrophil chemotaxis, degranulation, ROS production, and phagocytosis (43). FPR-1 was originally identified in phagocytic leucocytes and mediates cell chemotaxis and activation in response to the bacterial formylated chemotactic peptides (eg, fMLF). Agonist binding to FPR-1 elicits a signal transduction cascade involving phosphatidylinositol 3-kinase, protein kinase C (PKC), mitogen-activated protein kinases (MAPKs), and the transcription-factor NF-κB (44). Unlike FPR-1 that is expressed at high levels in both peripheral blood monocytes and neutrophils, FPR-2 is prevalently expressed in monocytes (44). Signals on both receptors can induce neutrophil recruitment to sites of inflammation, ROS production, degranulation, and cytokine release (41) as well as FPR signalling can induce an alternatively activated phenotype in macrophages which express IL-13, IL-4, and Arginase that utilizes arginine to produce proline, an essential iminoacid for collagen synthesis. Although FPRs were initially thought to bind only N-formylated peptides of bacterial origin (which are recognized as

potent pathogen-associated molecular patterns), FPRs also bind mitochondrial formylated peptides (damage-associated molecular patters) (45) released from cell after necrotic cell death, and other inflammatory non-formylated ligands which include cathepsin G, serum Amyloid A, and beta Amyloid or anti-inflammatory agonist such as annexin A1 and lipoxin A4 (41).

Recent studies indicate that formylated peptides, FPRs and in particular FPR-1 may be principal conductors in inflammatory processes in sterile-related (24, 26) and infection-related diseases (46). FPR-1 and formylated peptides, which are active components of cigarette smoke (47), have been recently involved in smoking-induced lung damage and studies performed in our laboratory demonstrated that *Fpr1*$^{-/-}$mice are protected from CS-induced emphysematous changes (24), suggesting that formylated peptides within cigarette smoke are central to disease pathogenesis. A similar beneficial reduction in inflammatory response, with fewer migrating neutrophils and macrophages and lower pro-inflammatory cytokine levels was observed after acute or sub-acute exposure to cigarette smoke (24). Further support for the role of FPRs in COPD pathogenesis have come from additional experimental studies in which alterations resembling COPD are induced in mice by a single intra-tracheal instillation of formylated peptides (31, 48).

Actually, these receptors are over-expressed in patients with COPD (25), and in established COPD, FPR activation by formyl-peptides released from mitochondria of necrotic cells or bacteria (that usually colonize pulmonary structures) may promote persistent inflammation by feeding the vicious cycle that causes persistent inflammation after smoking cessation.

In the present study, we demonstrate that selective inhibitors of FPR and FPR-1 exert therapeutic efficacy in an experimental animal model of COPD by halting the disease progression after smoking cessation. The inhibitor blockade of FPR-1 and FPR-1/FPR-2–related signalling can mitigate, after smoking cessation, the persistent inflammation and prevents the deterioration of pulmonary structures, which lead to airspace enlargement and airway remodelling.

The current study is the first to demonstrate a role for FPRs in persistent inflammation and in progressive lung destruction and maladaptive airways remodelling that follows smoking cessation in mice.

It also provides compelling rationale for FPR inhibition as a novel therapeutic strategy for treating COPD patients after smoking cessation.

References

1. Fabbri LM, Rabe KF: From COPD to chronic systemic inflammatory syndrome? Lancet 2007, 370:797-799
2. Mannino DM, Watt G, Hole D, Gillis C, Hart C, McConnachie A, Davey Smith G, Upton M, Hawthorne V, Sin DD, Man SF, Van Eeden S, Mapel DW, Vestbo J: The natural history of chronic obstructive pulmonary disease. Eur Respir J 2006, 27:627–643
3. Scanlon PD, Connett JE, Waller LA, Altose MD, Bailey WC, Buist AS, Tashkin DP; Lung Health Study Research Group**:** Smoking cessation and lung function in mild-to- moderate chronic obstructive pulmonary disease. Am J Respir Crit Care Med 2000, 161:381-390
4. Simmons MS, Connett JE, Nides MA, Lindgren PG, Kleerup EC, Murray RP, Bjornson WM, Tashkin DP: Smoking reduction and the rate of decline in FEV(1): results from the Lung Health Study. Eur Respir J 2005, 25:1011-1017
5. Willemse BW, ten Hacken NH, Rutgers B, Lesman-Leegte IG, Postma DS, Timens W**:** Effect of 1-year smoking cessation on airway inflammation in COPD and asymptomatic smokers. Eur Respir J 2005, 26:835-845
6. Gamble E, Grootendorst DC, Hattotuwa K, O'Shaughnessy T, Ram FS, Qiu Y, Zhu J, Vignola AM, Kroegel C, Morell F, Pavord ID, Rabe KF, Jeffery PK, Barnes NC: Airway mucosal inflammation in COPD is similar in smokers and ex-smokers: a pooled analysis. Eur Respir J 2007, 30:467-471
7. Lapperre TS, Postma DS, Gosman MM, Snoeck-Stroband JB, ten Hacken NH, Hiemstra PS, Timens W, Sterk PJ, Mauad T: Relation between duration of smoking cessation and bronchial inflammation in COPD. Thorax 2006, 61:115-121
8. Braber S, Henricks PA, Nijkamp FP, Kraneveld AD, Folkerts G: Inflammatory changes in the airways of mice caused by cigarette smoke exposure are only partially reversed after smoking cessation. Respir Res 2010, 11:99
9. Martorana PA, Cavarra E, Lucattelli M, Lungarella G: Models for COPD involving cigarette smoke. Drug Discov Today Dis Models 2006, 3:225–230
10. Rahman I, De Cunto G, Sundar IK, Lungarella G: Vulnerability and Genetic Susceptibility to Cigarette Smoke–Induced Emphysema in Mice. Am J Respir Cell Mol Biol 2017, 57:270-271
11. Tuder RM, Petrache I: Pathogenesis of chronic obstructive pulmonary disease. J Clin Invest 2012, 122:2749–2755
12. De Cunto G, Lunghi B, Bartalesi B, Cavarra E, Fineschi S, Ulivieri C, Lungarella G, Lucattelli M: Severe Reduction in Number and Function of Peripheral T Cells Does Not Afford Protection toward Emphysema and Bronchial Remodeling Induced in Mice by Cigarette Smoke. Am J Pathol 2016, 186:1814-1824
13. Churg A, Manuel C, Wright J: Mechanisms of cigarette smoke-induced COPD: insights from animal models. Am J Physiol Lung Cell Mol Physiol 2008, 294:L612-L631
14. Lucattelli M, Bartalesi B, Cavarra E, Fineschi S, Lunghi B, Martorana PA, Lungarella G: Is neutrophil elastase the missing link between emphysema and fibrosis? Evidence from two mouse models. Respiratory Research 2005, 6:83.

15. Rahman I, Adcock IM: Oxidative stress and redox regulation of lung inflammation in COPD. Eur Respir J 2006, 28:219-242

16. MacNee W, Rahman I: Oxidants and antioxidants as therapeutic targets in chronic obstructive pulmonary disease. Am J Respir Crit Care Med 1999, 160:S58-S65

17. Rossi R, Giustarini D, Fineschi S, De Cunto G, Lungarella G, Cavarra E: Differential thiol status in blood of different mouse strains exposed to cigarette smoke. Free Radical Res 2009, 43:538-545

18. Curtis JL, Freeman CM, Huffnagle GB: "B" for Bad, Beneficial, or Both? Lung Lymphoid Neogenesis in Chronic Obstructive Pulmonary Disease. Am J Respir Crit Care Med 2015, 192: 648–651

19. Calverley PM, Anderson JA, Celli B, Ferguson GT, Jenkins C, Jones PW, Yates JC, Vestbo J; TORCH investigators: Salmeterol and fluticasone propionate and survival in chronic obstructive pulmonary disease. N Engl J Med 2007, 356:775-789

20. Hatzelmann A, Morcillo EJ, Lungarella G, Adnot S, Sanjar S, Beume R, Schudt C, Tenor H **:** The preclinical pharmacology of roflumilast-A selective, oralphosphodiesterase 4 inhibitor in development for chronic obstructive pulmonary disease. Pulmonary Pharmacol & Therapeutics 2010, 23:235-256

21. Churg A, Tai H, Coulthard T, Wang R, Whright JL: Cigarette smoke drives small airway remodeling by induction of growth factors in the airway wall. Am J Respir Crit Care Med 2006, 174:1327–1334

22. Bartalesi B, Cavarra E, Fineschi S, Lucattelli M, Lunghi B, Martorana PA, Lungarella G: Different lung responses to cigarette smoke in two strains of mice sensitive to oxidants. Eur Respir J 2005, 25:15–22

23. De Cunto G, Cardini S, Cirino G, Geppetti P, Lungarella G, Lucattelli M: Pulmonary hypertension in smoking mice over-expressing protease-activated receptor-2. Eur Respir J 2011, 37:823–834

24. Cardini S, Dalli J, Fineschi S, Perretti M, Lungarella G, Lucattelli M: Genetic Ablation of the Fpr1 Gene Confers Protection from Smoking-Induced Lung Emphysema in Mice. Am J Respir Cell Mol Biol 2012, 47:332–339

25. Stockley RA, Grant RA, Llewellyn-Jones CG, Hill SL, Burnett D: Neutrophil formyl-peptide receptors: relationship to peptide-induced responses and emphysema. Am J Respir Crit Care Med 1994, 149:464–468

26. Dorward DA, Lucas CD, Doherty MK, Chapman GB, Scholefield EJ, Conway Morris A, Felton JM, Kipari T, Humphries DC, Robb CT, Simpson AJ, Whitfield PD, Haslett C, Dhaliwal K, Rossi AG: Novel role for endogenous mitochondrial formylated peptide-driven formyl peptide receptor 1 signalling in acute respiratory distress syndrome. Thorax 2017, 72:928–936

27. Martorana PA, Beume R, Lucattelli M, Wollin L, Lungarella G: Roflumilast Fully Prevents Emphysema in Mice Chronically Exposed to Cigarette Smoke. Am J Respir Crit Care Med 2005, 172:848–853

28. Cosio M, Ghezzo H, Hogg JC, Corbin R, Loveland M, Dosman J, Macklem PT: The relations between structural changes in small airways and pulmonary-function tests. N Engl J Med 1978, 298:1277-1281

29. Hasegawa M, Nasuhara Y, Onodera Y, Makita H, Nagai K, Fuke S, Ito Y, Betsuyaku T, Nishimura M: Airflow limitation and airway dimensions in chronic obstructive pulmonary disease. Am J Respir Crit Care Med 2006, 173:1309-1315

30. Cavarra E, Bartalesi B, Lucattelli M, Fineschi S, Lunghi B, Gambelli F, Ortiz LA, Martorana PA, Lungarella G: Effects of cigarette smoke in mice with different levels of alpha(1)-proteinase inhibitor and sensitivity to oxidants. Am J Respir Crit Care Med 2001, 164:886-980
31. Atzori L, Lucattelli M, Scotton CJ, Laurent GJ, Bartalesi B, De Cunto G, Lunghi B, Chambers RC, Lungarella G: Absence of Proteinase Activated Receptor-1 Signaling in Mice Confers Protection from fMLP-induced Goblet Cell Metaplasia. Am J Respir Cell Mol Biol 2009, 41: 680-687
32. Lucattelli M, Fineschi S, Selvi E, Garcia Gonzalez E, Bartalesi B, De Cunto G, Lorenzini S, Galeazzi M, Lungarella G: Ajulemic acid exerts potent anti-fibrotic effect during the fibrogenic phase of bleomycin lung. Respir Res. 2016, 6;17(1):49
33. Winer J, Jung CK, Shackel I, Williams PM. Development and validation of real-time quantitative reverse transcriptase-polymerase chain reaction for monitoring gene expression in cardiac myocytes in vitro. Anal Biochem 1999, 270: 41-49
34. Pahl HL. NF-kB activators and target genes of Rel/NF-kB transcription factors. Oncogene 1999, 18; 6853-6866
35. Hol J, Wilhelmsen L, Haraldsen G. The murine IL-8 homologues KC, MIP-2, and LIX are found in endothelial cytoplasmic granules but not in Weibel-Palade bodies. J Leukoc Biol 2010, 87: 501–508
36. Menten P, Wuyts A, Van Damme J. Macrophage inflammatory protein-1. Cytokine & Growth Factors Reviews. 2002; 6;455-481
37. Lunghi B, De Cunto G, Cavarra E, Fineschi S, Bartalesi B, Lungarella G, Lucattelli M: Smoking p66Shc knocked out mice develop respiratory bronchiolitis with fibrosis but not emphysema. Plos One 2015, 10; e0119797
38. Yu C, Wang F, Jin C, Huang X, Miller DL, Basilio C, McKean WL Role of fibroblast growth factor type 1 and 2 in carbon tetrachloride-induced hepatic injury and fibrogenesis. Am J Pathol 2003,163:1653-1662
39. Hautamaki RD, Kobayashi DK, Senior RM, Shapiro SD. Requirement for macrophage elastase for cigarette smoke-induced emphysema in mice. Science 1997, 227:2002-2004
40. Atherton HC, Jones G, Danahay H. IL-13–induced changes in goblet cell density of human bronchial epithelial cell cultures: MAP kinase and phosphatidylinositol 3-kinase regulation. Am J Physiol Lung Cell Mol Physiol 2003, 285;L730–L739.
41. Doward DA, Lucas CD, Chapman GB, Haslett C, Dhaliwal K, Rossi AG. The Role of Formylated Peptides and Formyl Peptide Receptor 1 in Governing Neutrophil Function during Acute Inflammation. Am J Pathol 2015, 185;1172-1184
42. Chen K, Bao Z, Gong W, Tang P, Yoshimura T, Wang JM. Regulation of inflammation by members of the formyl-peptide receptor family. Journal of Autoimmunity 2017, 85; 64-77
43. Gao JL, Chen H, Filie JD, Kozak CA, Murphy PM: Differential expansion of the N-formylpeptide receptor gene cluster in human and mouse. Genomics 1998, 51:270e276
44. Le Y, Yang Y, Cui Y, Yazawa H, Gong W, Qui C, Wang JM.Receptors for chemotactic formyl peptides as pharmacological targets. Int Immunopharmacol 2002, 2;1-13
45. Rabiet MJ, Huet E, Boulay F: Human mitochondria-derived N-formylated peptides are novel agonists equally active on FPR and FPRL1, while Listeria monocytogenes-derived peptides preferentially activate FPR. Eur J Immunol 2005, 35:2486–2495
46. Grommes J, Drechsler M, Soehnlein O: CCR5 and FPR1 mediate neutrophil recruitment in endotoxin-induced lung

injury. J Innate Immun 2014, 6:111–116

47. Hasday JD, Bascom R, Costa JJ, Fitzgerald T, Dubin W: Bacterial endotoxin is an active component of cigarette smoke. Chest 1999, 115:829e835
48. Cavarra E, Martorana PA, de Santi M, Bartalesi B, Cortese S, Gambelli F, Lungarella G: Neutrophil influx in the lung of Beige mice is followed by elastolytic damage and emphysema. Am J Respir Cell Mol Biol 1999, 20:264–269

Figure Legends

Fig. 1. Scheme of the experimental design of the study. The day of the start of the study was defined as day 0, allowing the association of this time point with the schedule of smoke cessation and compound administration. Red arrow: day 0, the day of the start of the study. CS: cigarette smoke. SC: smoke cessation. Boc2: N-t-butoxycarbonyl-Phe-DLeu-Phe-DLeu-Phe-OH. CsH: cyclosporine H. Blue arrows: time point at which mice received pharmacological treatment. Blue line: time period in which mice were left to rest at room air after smoking cessation. Roman cross: time of the sacrifice; mice from Groups 3-5 were first sacrificed at 4 months plus 8 days after the start of the study.

Fig. 2. Lung Morphology. Histology at four months from the start of the study. Representative histologic sections from lungs of mice at four months after air **(A)** or CS **(B)** exposure. Histologic section of lung from a control mouse at four months from the start of the study showing a normal parenchyma **(A**). **B:** A representative histologic section from a mouse at four months after CS exposure showing disseminated mild foci of emphysema. Hematoxylin and eosin staining. Scale bars = 120 μm. Mean linear intercepts (LM) values (**C**) and internal surface areas (ISA) **(D)** in lungs of mice exposed (CS 4M) or not exposed (Air 4M) to CS. **P* <0.05 vs air control mice.

Fig. 3. Lung Morphology. Histology at 10 months from the start of the study. Representative histologic sections from lungs of mice at 10 months after air **(A)** or CS exposure **(B). C:** Lung from a mouse exposed for four months to CS and then left to rest after smoking cessation at room air for six months. Evident areas of emphysema are present scattered throughout the parenchyma. Representative histologic sections of mice treated with Boc2 or CsH, at the time of smoking cessation and left to rest at room air for six months are shown in **D** and **E**, respectively. Hematoxylin and eosin staining. Scale bars = 120 μm. **F:** Mean linear intercepts (LM) values and internal surface areas (ISA) in lungs of mice exposed for 10 months to room air (Air), to CS (CS) or exposed for four months to CS and left to rest after smoking cessation at room air for six months (SC). (BOC) and (CsH) indicate mouse groups treated at the time of smoking cessation with Boc2 or CsH, respectively, and left to rest at room air for six months. **P* <0.05 vs air control mice; $^{\dagger}P$ < 0.05 vs CS-exposed mice (CS); $^{\ddagger}P$ < 0.05 vs smoking cessation group (SC).

Fig. 4. Inflammatory cells in lung tissues at 10 months and in BALFs at eight months from the start of the study. Representative histologic sections from lungs of mice at 10 months after air

exposure **(A)** in which inflammatory cells are virtually absent. At 10 months following chronic smoke exposure **(B)** inflammatory cells are present throughout lung parenchyma. The lungs of ex-smoking mice after SC mice observed at 10 months are also characterized by a persistent accumulation of inflammatory cells in lung tissue **(C)**. Very few inflammatory cells are present in lung parenchyma of mice receiving a treatment with Boc2 **(D)** or CsH **(E)**. Hematoxylin and eosin staining. Scale bars = 40 μm.

Fig. 5. Nuclear translocation of NF-kB and real-time PCR analysis of mRNAs for some NF-kB target genes encoding for pro- or anti-inflammatory cytokines and chemokines. A: Immunohistochemical reaction (green staining) for NF-kB in lung section from air-control mouse. In this group of mice, NF-kB in its inactive status is localized in the cytoplasm of macrophages and alveolar cells. **B:** Lung section from a mouse exposed for six months to CS. NF-kB can be observed in the nuclei of several macrophages and alveolar cells (arrowheads). **C:** Nuclear localization of NF-kB (green staining) can be appreciated also in lung slides from mice exposed for four months to CS and then left to rest after smoking cessation at room air for two months (arrowheads). **D** and **E:** No nuclear localization of NF-kB can be seen in lung histologic sections of mice treated with Boc2 **(D)** or CsH **(E)**, at the time of smoking cessation and left to rest at room air for two months. **A-E:** Scale bars = 20 μm. **F:** Real-time PCR analysis of mRNAs for macrophage inflammatory protein1beta (*Ccl4*//MIP-1), interleukin 6 (*Il6*), cytokine-induced neutrophil-attracting chemokine (*Cxcl1*/KC), and *Il10* performed on lungs from five mice for each experimental group at six months from the start of experiments. Values are corrected for 18S rRNA and normalized to a median control value of 1.0. Data are presented as mean ± SD. **P* < 0.05 compared with air-control values; †*P* <0.05 vs SC group.

Fig. 6. Lung Morphology. Airway morphology: Peribronchiolar fibrosis. Histologic sections from distal airways after Masson's trichrome staining. **A:** Distal airway of an air-exposed mouse showing a normal appearance. **B:** Peribronchiolar region of a mouse at 10 months after CS exposure thickened by an evident fibrotic reaction. Note a large number of inflammatory cells in peribronchiolar area. **C:** Tissue section of a smoking mouse at four months of exposure showing a mild increase of collagen (sea-green stain) around a distal airway. Inflammatory cells are present in surrounding areas. **D:** Collagen is markedly increased in peribronchiolar spaces of mice exposed for four months to CS and then left to rest after smoking cessation at room air for six months. Inflammatory cells are still present in peribronchiolar spaces. Peribronchiolar spaces of mice at six months after smoking cessation that received Boc2 **(E)** or CsH **(F)** at four months of CS-exposure.

Minimal differences in sea-green–stained areas are observed between the latter groups of mice and those sacrificed at four months of smoke exposure **(C)**. Masson's trichrome stain. Scale bars = 40 μm.

Fig. 7. Masson's trichrome–stained areas, real-time PCR analysis of mRNAs for some NF-kB target genes, quantification of goblet cell metaplasia in lungs of mice from various experimental groups at 10 months from the start of the study. A: Data are reported as values of sea green area/micrometer length of basement membrane of bronchioles 150 to 300 mm of internal diameter at 10 months from the start of the study. Data are presented as mean ± SD. Air = air exposure; CS 10M = cigarette smoke exposure; CS+SC= cigarette smoke plus smoke cessation; Boc2= Boc2 treatment after SC; CsH = CsH treatment after SC. Animal number = 6 in all groups. $^{*}P$ <0.05 vs air exposed mice; $^{\dagger}P$ < 0.05 vs CS-exposed mice; $^{\ddagger}P$ < 0.05 vs SC group. **B:** Real-time PCR analysis of mRNAs for protease-activated receptor-1 (PAR-1, *F2r*), fibroblast growth factor-1 (*Fgf1*), interleukin 13 (*Il13*), arginase-1 (*Arg1*), and macrophage metalloprotease-12 (Mmp12) performed on lungs from five mice for each experimental group at eight months from the start of experiments. Values are corrected for 18S rRNA and normalized to a median control value of 1.0. Data are presented as mean ± SD. $^{*}P$ < 0.05 vs air-control values; $^{\dagger}P$ <0.05 vs SC group. **C:** Number of PAS positive cells per millimeter of basement membrane. **D:** Percentage of PAS positive cells per total cells**.** At six months after smoking cessation mice which received Boc2 or CsH at four months of CS-exposure showed a marked significant reduction of PAS-positive cells in airway epithelium. Each bar represents the mean ± SD. $^{*}P$ < 0.05 vs CS group at 10 Months; $^{\dagger}P$ <0.05 vs SC group. **E:** Lung from air control mouse, no PAS positive cells are present in tissue sections. **F:** Lung from CS-exposed mouse at 10 months showing a large number of goblet cells in the epithelium of bronchioles and in middle-sized bronchi. **G:** Goblet cell metaplasia can be appreciated in airways epithelium of CS-exposed mice also at four months from the start of the study. **H:** Significant areas of goblet cell metaplasia can be appreciated in airway epithelium of ex-smoker mice at six months from SC. At six months after smoking cessation mice which received Boc2 **(I)** or CsH **(J)** at four months of CS-exposure showed only few scattered goblet cells in the epithelium of bronchioles and middle-sized bronchi (arrowheads). PAS stain. Scale bars = 100 μm.

Table 1. Primers Sequence and Probe Catalog Number.

Primer name	Primer sequence	Probe
KC (CXCL1)	Forward 5′- AGACTCCAGCCACACTCCAA -3′ Reverse 5′- TGACAGCGCAGCTCATTG -3′	18
IL-6	Forward 5′- ACAAAGCCAGAGTCCTTCAGA -3′ Reverse 5′- TGGTCCTTAGCCACTCCTTC -3′	78
IL-10	Forward 5′- CAGAGCCACATGCTCCTAGA -3′ Reverse 5′- TGTCCAGCTGGTCCTTTGTT -3′	41
MIP-1beta	Forward 5′- GCCCTCTCTCTCCTCTTGCT -3′ Reverse 5′- GGAGGGTCAGAGCCCATT -3′	1
MMP-12	Forward 5′-TTGTGGATAAACACTACTGGA GGT -3′ Reverse 5′- AAATCAGCTTGGGGTAAGCA -3′	51
Arg 1	Forward 5′- GAATCTGCATGGGCAACC -3′ Reverse 5′- GAATCCTGGTACATCTGGGAA -3′	2
FGF 1	Forward 5′- CAGCCTGCCAGTTCTTCAG -3′ Reverse 5′- GGCTGCGAAGGTTGTGAT -3′	41
IL-13	Forward 5′- CCTCTGACCCTTAAGGAGCTTAT-3′ Reverse 5′- CGTTGCACAGGGGAGTCT -3′	17
F2r(PAR-1)	Forward5′-GTCTTCCCGCGTCCCTAT-3′ Reverse 5′- GGGTTCACCGTAGCATCTGT -3′	20
18S rRNA	Forward 5′-AAATCAGTTATGGTTCCTTTGGTC-3′ Reverse 5′-GCTCTAGAATTACCACAGTTATCCAA-3′	55

Table 2. Total and Differential Cell Count in BALFs after Eight Months from the Start of the Study.

	Air-exposed	Smoke-exposed	Smoke cessation
Total cell count, x10^5	**1.35±0.4**	**1.96±0.43***	**1.50±0.14**
Differential cell count, x10^5			
Macrophages	**1.13±0.3**	**1.36±0.35**	**1.11±0.11**
Neutrophils	**0.14±0.05**	**0.46±0.11***	**0.30±0.04*†**
Lymphocytes	**0.08±0.04**	**0.14±0.04**	**0.09±0.01†**

*$P < 0.05$ vs
†$P < 0.05$ vs smoke- exposure.
Data are given as mean± SD from 5 mice/group. They represent data from mice exposed for eight months to air, cigarette smoke, or mice left to rest for four months to room air after smoke cessation. The slides were stained with Diff Quick©.

Table 3. Total and Differential Cell Count in BALFs at 4 Months and 8 Days after the Start of the Study.

	Air	Smoke	Smoke cessation	Smoke cessation+ Boc2	Smoke cessation+ CsH
Total cell count, x10^5	**0.96±0.16**	**1.6±0.19***	**1.49±0.21***	**1.15±0.08*†**	**1.10±0.25†**
Differential cell count, x10^5					
Macrophages	**0.82±0.15**	**1.13±0.16***	**1.07±0.14***	**0.95±0.09**	**0.92±0.22**
Neutrophils	**0.08±0.02**	**0.34±0.04***	**0.29±0.05***	**0.12±0.01*†**	**0.10±0.03†**
Lymphocytes	**0.06±0.01**	**0.13±0.01***	**0.14±0.03***	**0.08±0.02*†**	**0.08±0.02*†**

$^*P < 0.05$ vs air-exposure.
$^\dagger P < 0.05$ vs smoke- exposure.
Data are given as mean± SD from 5 mice/group. They represent data from animals exposed to air, cigarette smoke, or exposed to cigarette smoke for four months and left to rest for eight days in room air after smoke cessation. The last groups of mice received FPRs antagonists after smoking cessation. The slides were stained with Diff Quick©.
Boc2, N-t-butoxycarbonyl-Phe-DLeu-Phe-DLeu-Phe-OH; CsH, cyclosporine H.

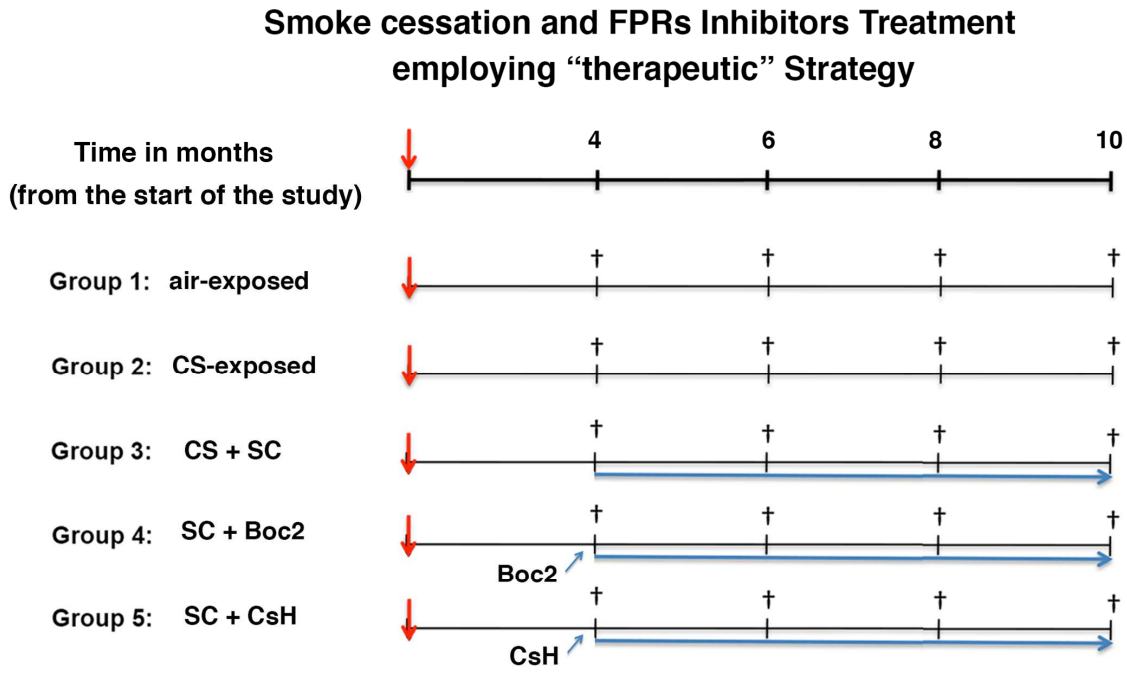

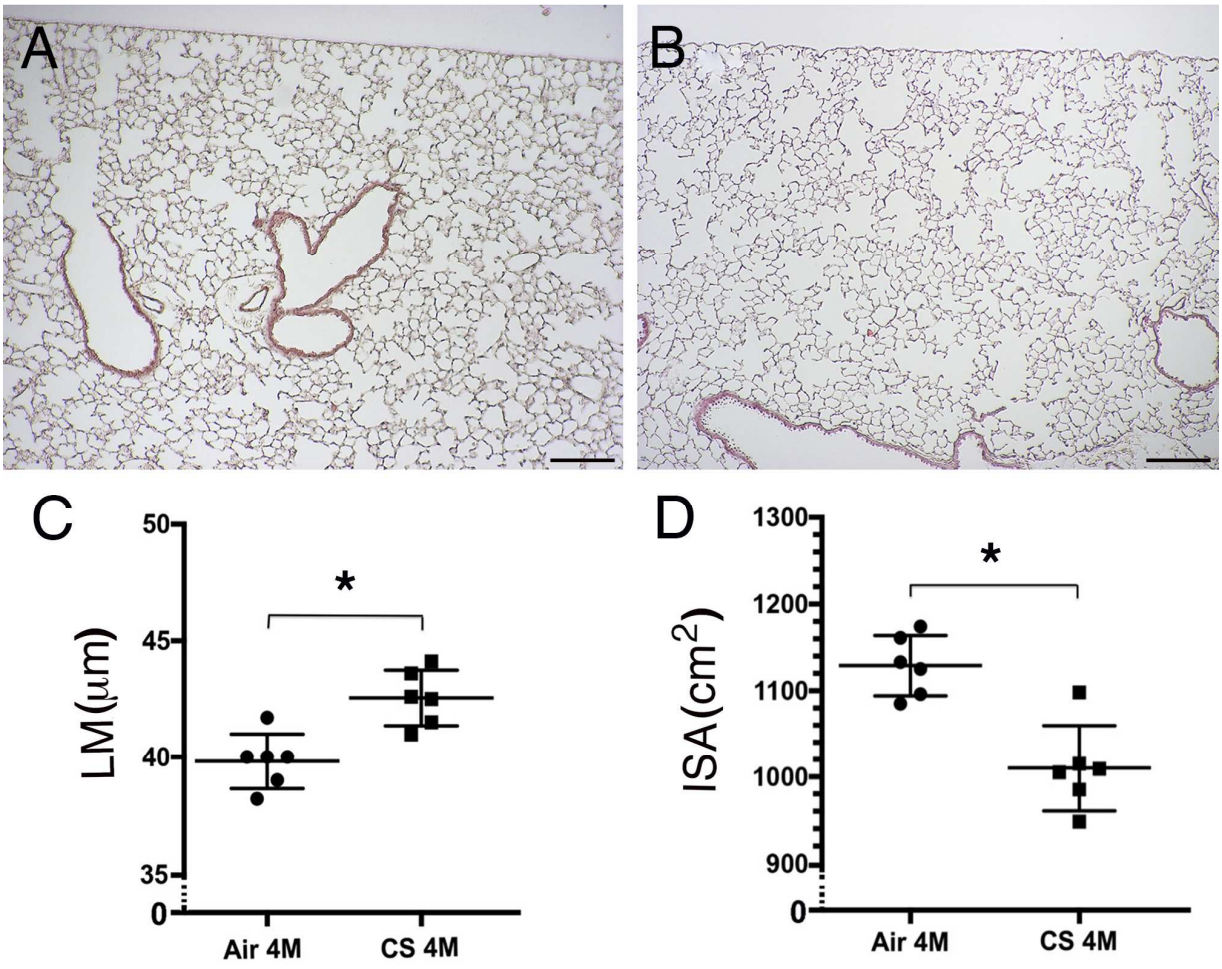
A
B
C
LM(μm)
50
45
40
35
0
*
Air 4M
CS 4M
D
ISA(cm2)
1300
1200
1100
1000
900
0
*
Air 4M
CS 4M

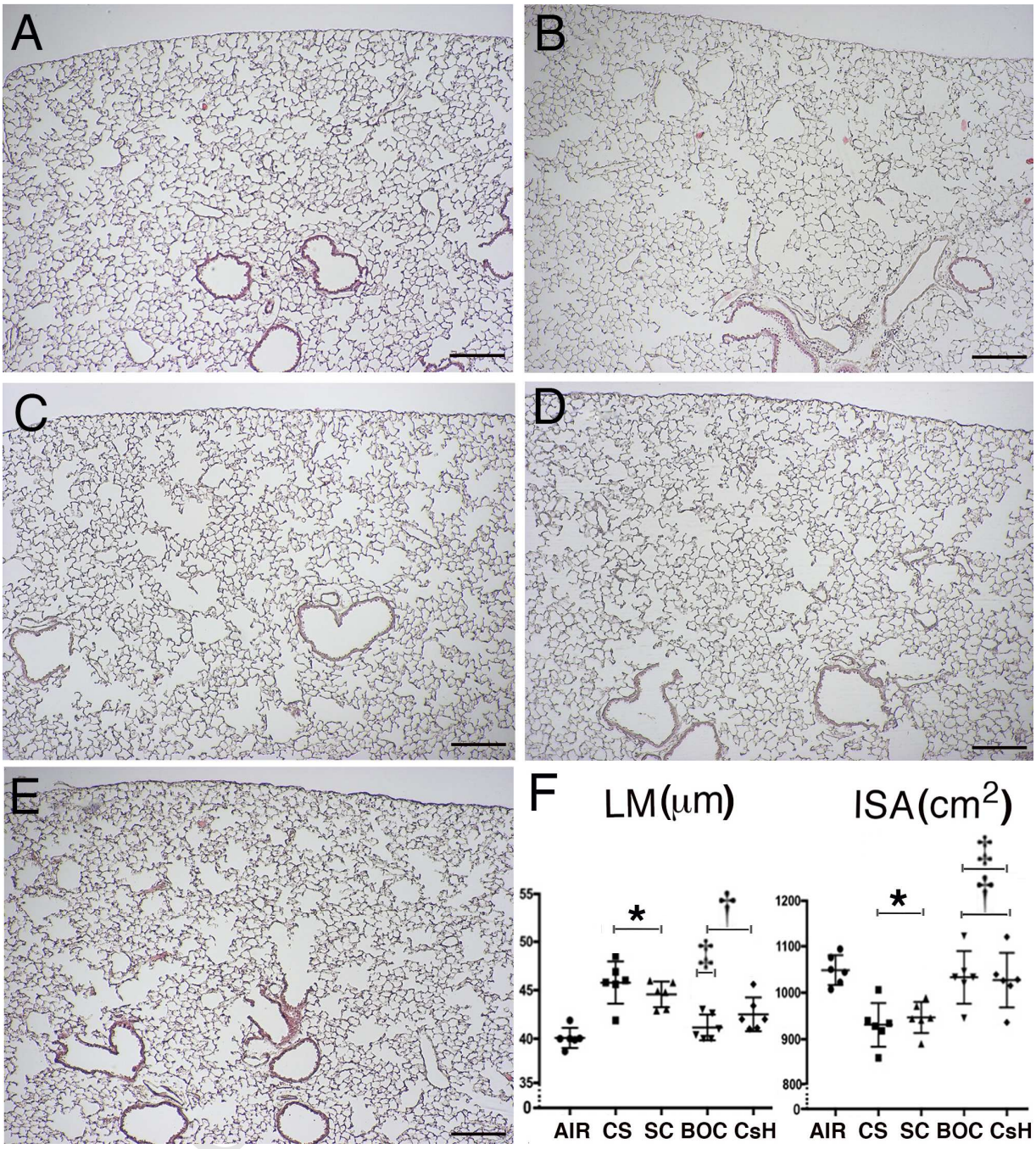
A
B
C
D
E
F
LM(μm)
ISA(cm²)
55
50
45
40
35
0
1200
1100
1000
900
800
0
*
*
AIR CS SC BOC CsH
AIR CS SC BOC CsH

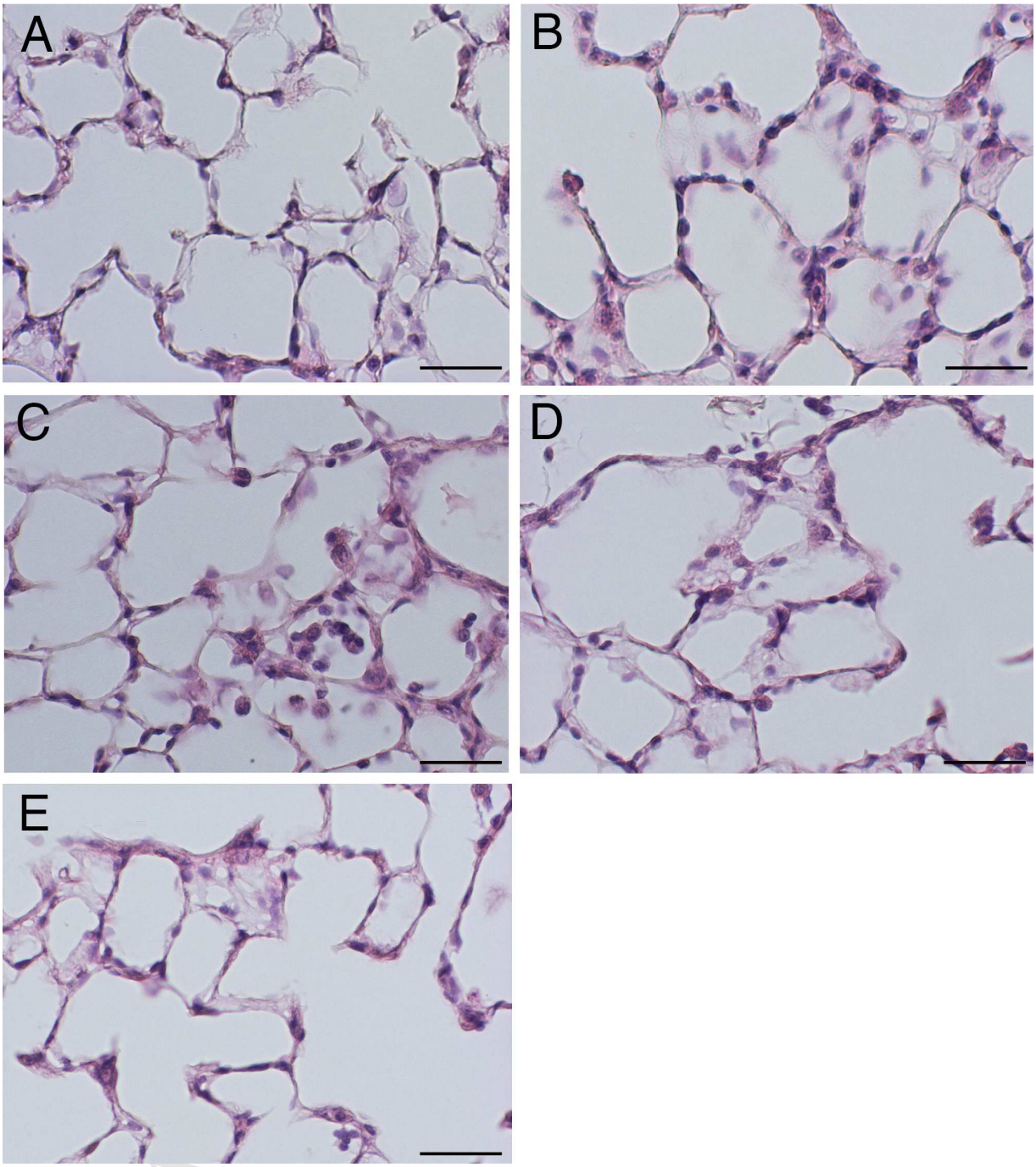
A
B
C
D
E

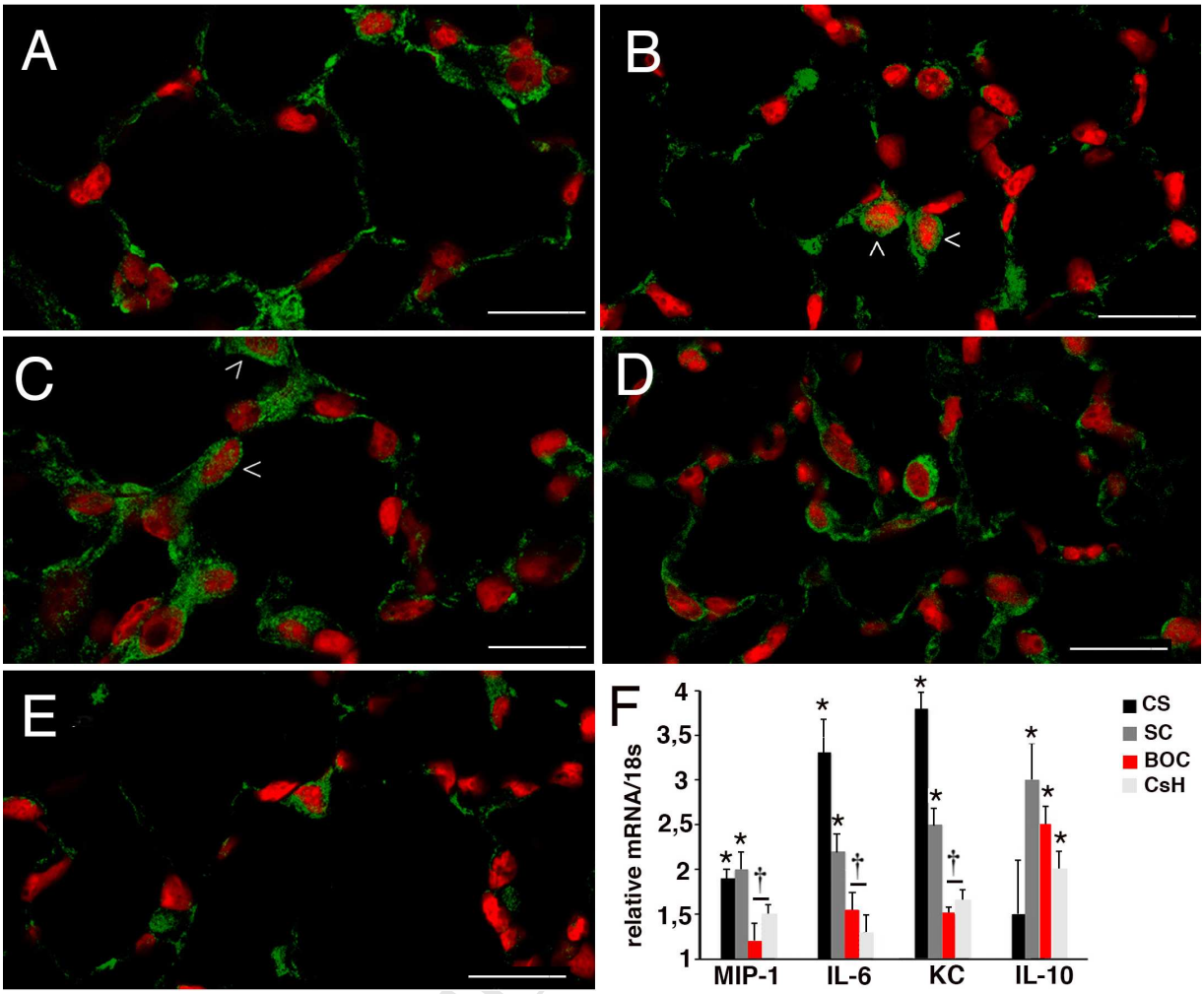

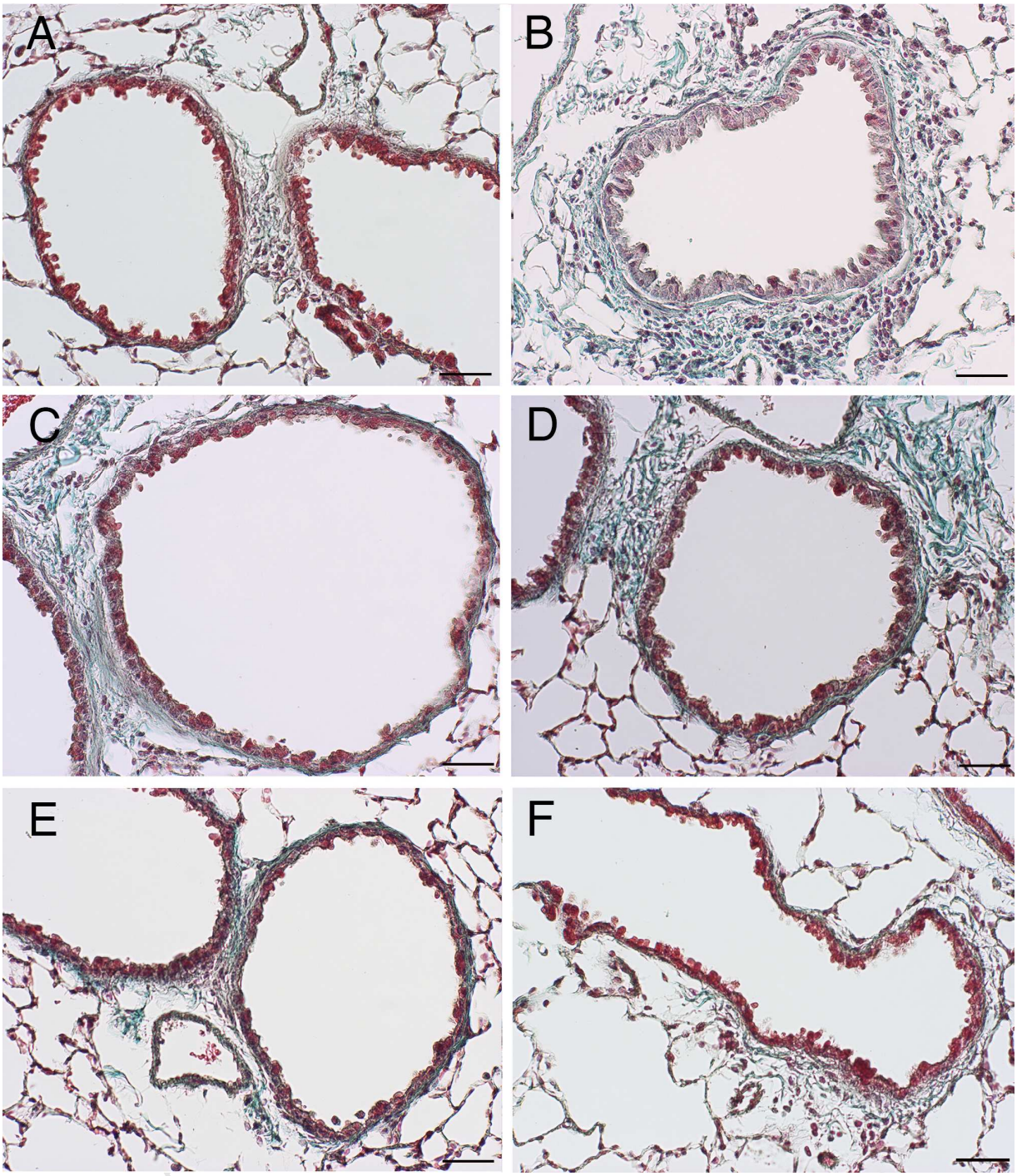
A
B
C
D
E
F

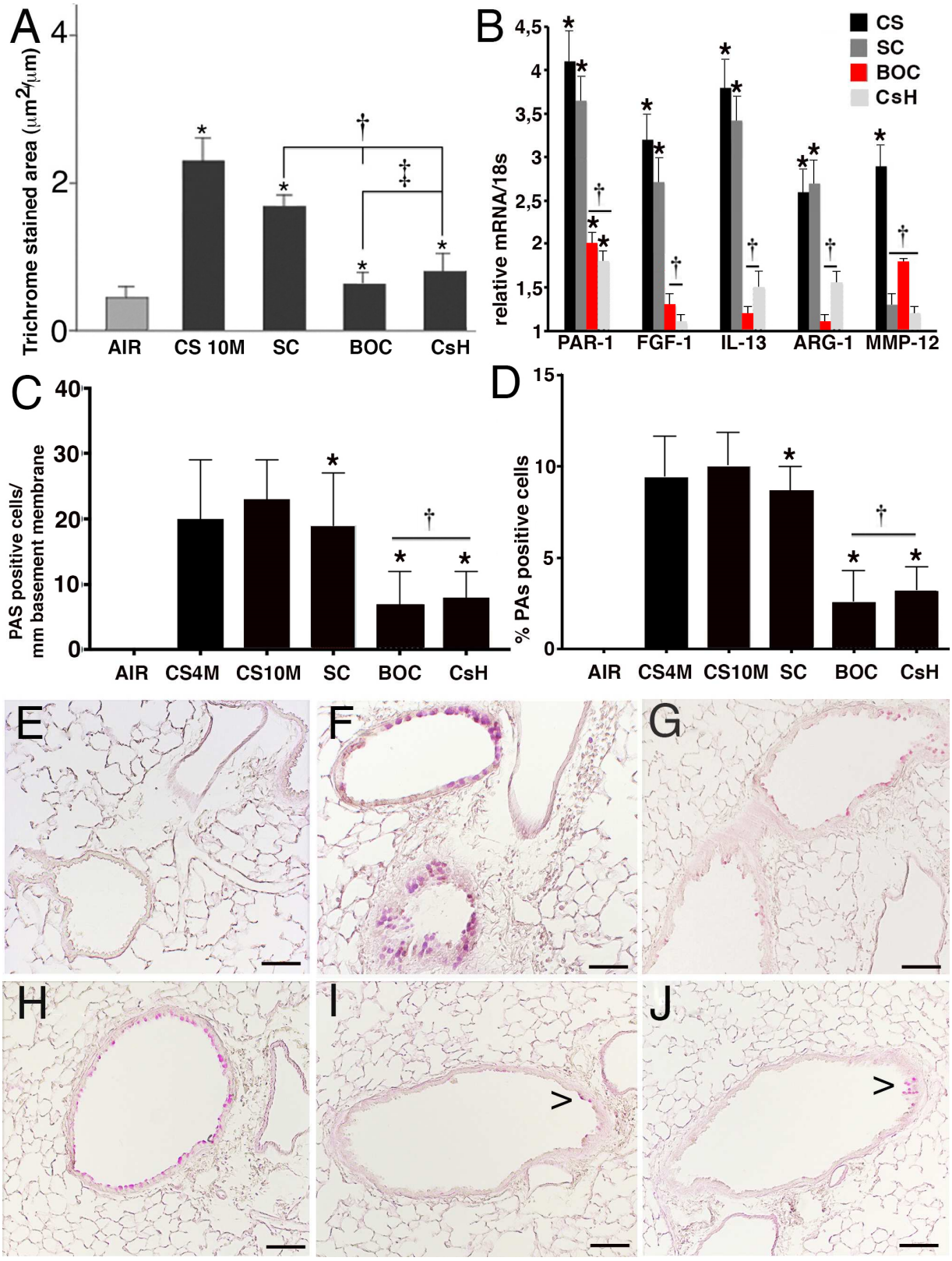
A
Trichrome stained area (μm²/μm)
AIR
CS 10M
SC
BOC
CsH
B
relative mRNA/18s
CS
SC
BOC
CsH
PAR-1
FGF-1
IL-13
ARG-1
MMP-12
C
PAS positive cells/ mm basement membrane
AIR
CS4M
CS10M
SC
BOC
CsH
D
% PAs positive cells
AIR
CS4M
CS10M
SC
BOC
CsH
E
F
G
H
I
J